JOURNAL

OF THE AMERICAN CHEMICAL SOCIETY

VOLUME 103, NUMBER 4 FEBRUARY 25, 1981

Secondary Ion Mass Spectrometry of Small-Molecule Solids at Cryogenic Temperatures. 1. Nitrogen and Carbon Monoxide

Harry T. Jonkman and Josef Michl*

Contribution from the Department of Chemistry, University of Utah, Salt Lake City, Utah 84112. *Received July 23, 1980*

Abstract: Secondary ion mass spectra of solid nitrogen and carbon monoxide were observed at 15 K. The effects of the nature and energy of the primary probe ion were investigated. Direct charge transfer, inelastic momentum transfer, association reactions, and ion–molecule reactions all seem to contribute to the formation of the secondary charged particles. With the heavier probe ions extensive cluster formation was observed.

Introduction

The development of secondary ion mass spectrometry (SIMS) for the analysis of organic solids, polymers, and materials of biochemical interest has received increasing attention in recent years.[1] Since SIMS can be used for the study of high molecular weight nonvolatile and heat-sensitive materials, it seems to have the potential to extend the reach of mass spectrometric applications and to form a valid alternative for methods like plasma desorption mass spectrometry[2] and pyrolysis mass spectrometry.[3] An additional advantage is the extreme sensitivity of surface analysis methods in general.

So far, exploratory research has been conducted on a limited number of compounds such as amino acids and peptides,[4] neat and argon-diluted organics held at cryogenic temperatures,[5] and polymers.[6] More recent results have been published discussing cluster formation during ion bombardment of small molecular systems (frozen water and benzene[7] and frozen nitrogen and methane[8]).

All these studies show the occurrence of ion–molecule reactions, cluster formation, and more extensive fragmentation compared with electron-impact mass spectrometry. These phenomena are of considerable potential interest. For example, a study of charged clusters may help in the understanding of solvated ion–solvent interactions, especially because clusters of almost any size can be formed. A study of ion–molecule reactions in SIMS would complement the results for similar reactions in ion cyclotron resonance (ICR) and crossed-beam experiments because it represents a situation of a very dense target medium with a very high collision cross section.

On the other hand, the relatively high degree of fragmentation and the low yield of the parent ion represent a complication in analytical applications of SIMS. The high fragmentation upon impact often makes the spectra of members of a homologous series nearly identical, as was shown for neat methane, propane, and pentane.[5,8]

Theoretical and experimental efforts have been made by several groups to obtain a better understanding of the underlying mechanism of ionization, sputtering, and cluster formation.[1] Although some insight has been gained, much remains to be understood.

In order to make further progress, we undertook a study of very small molecules frozen as solids at cryogenic temperatures. Small molecules were selected in order to simplify the fragmentation patterns. In this paper we will present results of SIMS experiments on samples of solid nitrogen and carbon monoxide.

Experimental Section

The spectra were measured on a home-built instrument constructed from commercially available components. The ultrahigh vacuum (UHV)

(1) *Springer Ser. Chem. Phys.* **9** (1979); R. J. Day, S. E. Unger, and R. G. Cooks, *Anal. Chem.*, *52*, 557A (1980).
(2) D. F. Torgerson, R. P. Skowronski, and R. D. Macfarlane, *Biochem. Biophys. Res. Commun.*, *60*, 616–21 (1974).
(3) H. L. C. Meuzelaar, P. G. Kistemaker, and M. A. Posthumus, *Biomed. Mass Spectrom.*, *1*, 312–9 (1974).
(4) A. Benninghoven, *CRC Crit. Rev. Solid State Sci.*, 291–316 (1976); *Surf. Sci.*, **35**, 427–57 (1973); H. Grade, N. Winograd, and R. G. Cooks, *J. Am. Chem. Soc.*, **99**, 7725–6 (1977); F. W. Karasek, *Res./Dev.*, **25** (11), 42–8 (1974); F. M. Devienne and J. Giroud, *C. R.—Symp. Int. Jets Mol.*, 5th, 1975, paper no. B7; *Chem. Abstr.*, **87**, 126687, 1977; A. Benninghoven, D. Jaspers, and W. Sichtermann, *Appl. Phys.*, **11**, 35–9 (1976); A. Benninghoven and W. Sichtermann, *Org. Mass Spectrom.*, **12**, 595–7 (1977); H. Grade, R. J. Day, and R. G. Cooks, Abstracts, 29th Pittsburgh Conference on Analytical Chemistry and Applied Spectroscopy, Cleveland, Ohio, Feb 27–Mar 3, 1978, p 383.
(5) H. T. Jonkman and J. Michl, *J. Chem. Soc., Chem. Commun.*, 751–2 (1978); H. T. Jonkman, J. Michl, R. N. King, and J. D. Andrade, *Anal. Chem.*, **50**, 2078–82 (1978).
(6) J. A. Gardella and D. M. Hercules, *Anal. Chem.*, **52**, 226–32 (1980); G. D. Tantsyrev and N. A. Kleimenov, *Dokl. Akad. Nauk SSSR*, **213**, 649–52 (1973); G. D. Tantsyrev and M. I. Povolotskaya, *Khim. Vys. Energ.*, **9**, 380–3 (1975); G. D. Tantsyrev, N. A. Kleimenov, M. I. Povolotskaya, and N. M. Bravaya, *Vysokomol. Soedin., Ser. A*, **18**, 2218–22 (1976); G. D. Tantsyrev, M. I. Povolotskaya, and N. A. Kleimenov, *ibid.*, **19**, 2057–65 (1977); G. D. Tantsyrev and M. I. Povolotskaya, *Vzaimodeistvie At. Chastits Tverd. Telom Dokl. Vses. Konf., 3rd*, 219–22 (1974); *Ref. Zh., Khim.*, 1975, Abstr. No. 9S15.
(7) G. M. Lancaster, F. Honda, Y. Fukuda, and J. W. Rabalais, *J. Am. Chem. Soc.*, **101**, 1951–8 (1979).
(8) H. T. Jonkman and J. Michl in ref 1, pp 292–5.

0002-7863/81/1503-733$01.00/0

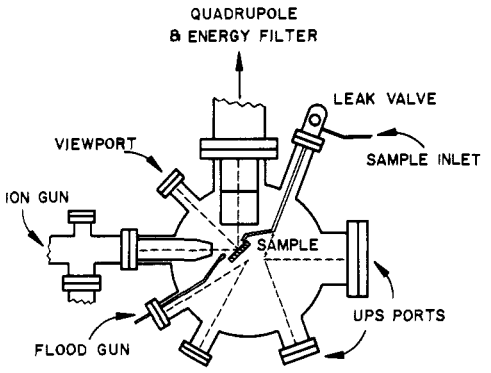

Figure 1. Schematic representation of the SIMS instrument.

chamber (Figure 1) was designed in such a way that one can perform SIMS as well as UPS experiments on the same sample by rotating the sample holder which is mounted 1 in. off-center in a 10-in.-diameter stainless steel UHV chamber. All seals are made by oxygen-free high-conductivity copper gasket sealed knife-edge flanges.

The main chamber is roughed by liquid nitrogen cooled sorption pumps and pumped down with a 500 L/s Vacion diode ion pump. With this arrangement a background pressure in the order of 10^{-10} torr can be maintained easily. A Riber CI50RB ion gun with scanning plates is used as a source of primary ions. This gun is differentially pumped with a 100 L/s turbomolecular pump and is able to produce beams with diameters between 0.1 and 3 mm, with ion current densities between 10^{-10} and 10^{-6} A/cm^2. The ion energy can be adjusted between 0.5 and 5.0 keV. The secondary ions are energy filtered by a Bessel box. The mass spectrometer is a quadrupole (Extranuclear) operated at ca. 1.6 MHz and has a mass range of 1000 amu. Both positive and negative ions can be detected in a direct-current and a pulse-counting mode.

The signal is collected in a 4096-channel Nicolet 1170 signal averager which also provides the ramp for the mass spectrometer. Because our samples are insulators, we use a current-regulated filament biased −5 V with respect to the sample plate as an electron floodgun. This compensates for a buildup of positive charge on the sample surface by ion bombardment. The sample plate is made of oxygen-free high-conductivity copper and is attached to the head of an Air Products Displex closed-cycle cryostat whose temperature can be adjusted between ambient and 10 K. The large cold surface of this cold probe also provides efficient cryopumping of the UHV chamber.

The ion probe gases were He, Ne, Ar, Kr, and Xe (Matheson Co., >99.95% purity). The purity of N_2 and CO was at least 99.5%. The samples were bled into the UHV chamber through a high-precision leak valve from a diffusion-pumped sample preparation system evacuable to background pressures below 10^{-6} torr. In most experiments more than 100 monolayers were deposited.

Results and Discussion

The samples were condensed on a sample plate held at 15 K and primary ion current densities below 10 nA/cm^2 were utilized, which means that phenomena associated with the simultaneous impact of several primary ions in the same region of the sample were not observed. The mass spectrometer was tuned for optimal resolution near 80 amu and the energy prefilter was set for transmission of ions with a bandwidth of ca. 1 eV. The electron floodgun was adjusted in the same way as reported before.[5] The spectra were quite reproducible, but the comparison of absolute yields between different experiments was often poor, as was observed before.[1]

Nitrogen. Figure 2 shows the SIMS spectrum of solid N_2 taken with a 4-keV argon ion beam. Here we observe N^+, N_2^+, N_3^+, N_4^+, and a large number of cluster ions with an odd or even number of nitrogen atoms up to the limit of the mass range of the spectrometer. The largest cluster observed contains 35 nitrogen molecules. These clusters can be thought of as consisting of N^+ and/or N_3^+ ions for the odd multiples and N_2^+ and/or N_4^+ ions for the even multiples, solvated by groups of neutral nitrogen

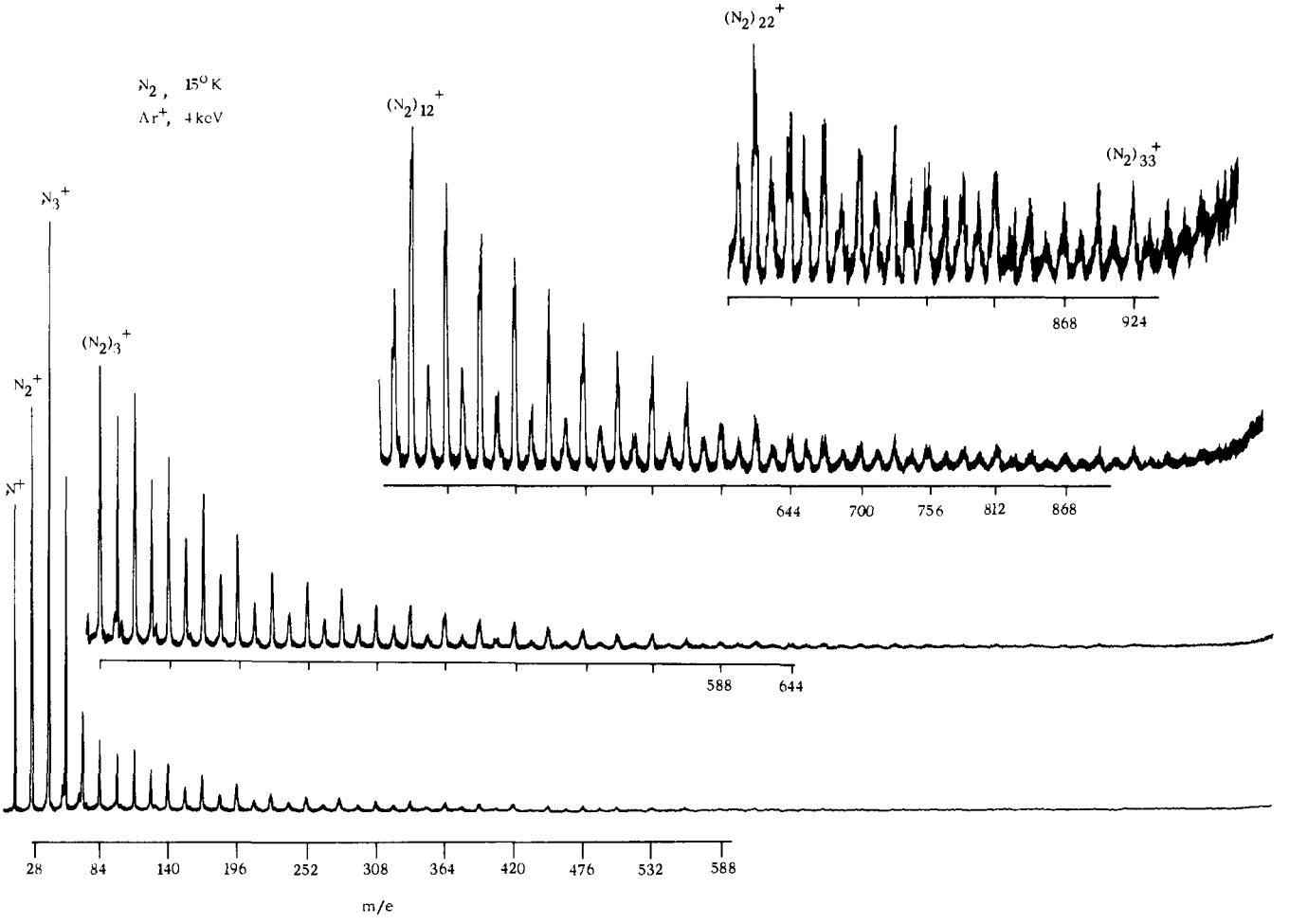

Figure 2. Positive SIMS spectrum of solid N_2 obtained with a 4-keV Ar^+ beam.

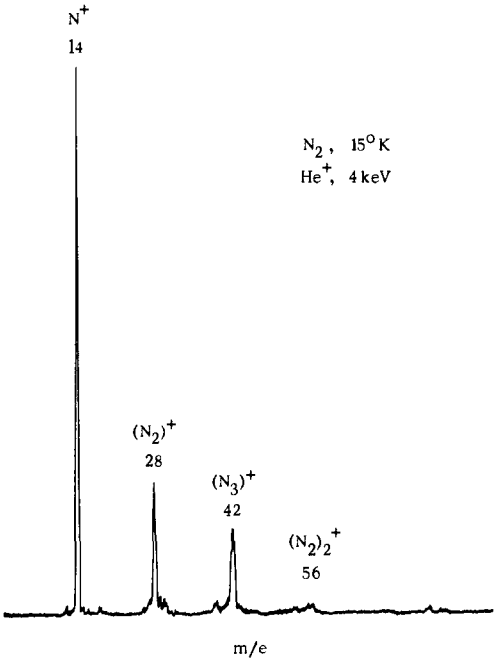

Figure 3. Positive SIMS spectrum of solid N_2 obtained with a 4-keV He^+ beam.

molecules. Figure 3 shows the SIMS spectrum of N_2 obtained with a 4-keV helium ion beam. Here only the N^+, N_2^+, N_3^+, and N_4^+ ions are present and there is virtually no cluster formation. The spectra obtained with Ne^+, Kr^+, and Xe^+ beams were similar to the one obtained with an Ar^+ ion beam. The total cluster yield and the average cluster size increase with the mass of the primary ion. An increase of the primary beam energy from 0.5 to 5.0 keV did not change the major features of the spectra but did enhance the cluster formation.

For a qualitative discussion of the above results, attention has to be paid to the possible events following the impact of a highly energetic inert gas ion on a molecular solid. Three consecutive events can be distinguished upon ion impact.

(i) If the ion is not reflected by the first monolayer, it penetrates into the solid and loses its kinetic energy through a cascade of collisions. At some time the ion will lose its charge to a molecule by charge transfer or undergo association reactions. This often creates an ion in a highly excited state which may fragment or undergo further ion–molecule reactions. Under certain conditions the primary ion may create secondary ions by combination of direct charge transfer and inelastic momentum transfer or by inelastic momentum transfer by itself, although cross sections of this last process are not very large.[9]

(ii) Upon ion impact and the following collision cascade many molecules acquire an excess of kinetic energy and a highly disturbed thermally activated region is formed in the solid, which perhaps behaves as if it were dense gas. The energetic secondary ions travel through this region on their way out and may undergo association reactions or form clusters. These thermally activated clusters lose their energy by an expansion in the vacuum. We suspect that this causes a rapid cooling of the clusters and thus may be the reason for their stability. This cooling is conceivably related to the one observed with expansions through supersonic nozzles[10] and contrasts with the high vibrational temperatures (ca. 5000 K) observed for negative ions containing up to five atoms, sputtered off metal targets by 4-keV Cs^+ ions.[11] Any further

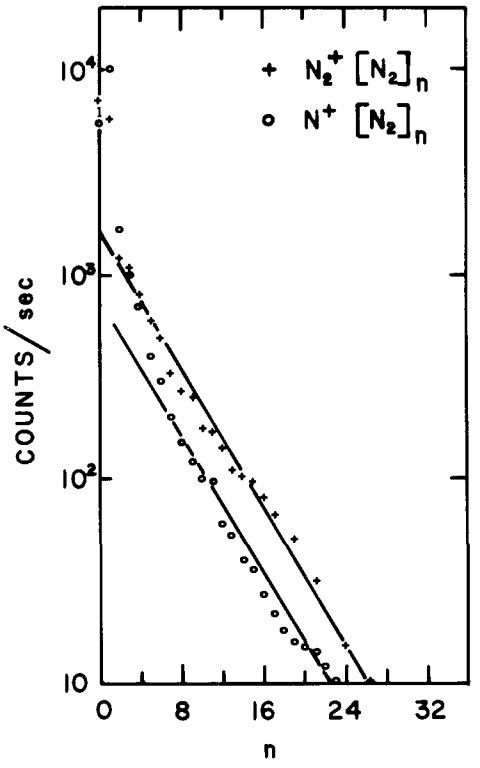

Figure 4. Cluster ion count rate as a function of the cluster size for solid N_2 bombarded with a 4-keV Ar^+ beam.

speculation appears unwarranted at present; rather, a more detailed picture ought to result from molecular dynamics calculations.

(iii) On their way through the spectrometer the ions and cluster ions may undergo further fragmentation or rearrangements and further cooling by partial vaporization.

For nitrogen, N^+, N_2^+, N_3^+, and N_4^+ ions will in general be formed by events described under i. The corresponding known charge-transfer reactions are[9]

N^+:	$N_2(X) \rightarrow N^+(^3P) + N + e^-$	AP = 24.3 eV
N_2^+:	$N_2(X) \rightarrow N_2^+(X) + e^-$	AP = 15.6 eV
N_3^+: a	$\begin{cases} N_2(X) \rightarrow N_2^+(^4\Sigma_u^+) + e^- \\ N_2^+(^4\Sigma_u^+) + N_2(X) \rightarrow N_3^+ + N \end{cases}$	AP = 22.6 eV
b	$\begin{cases} N_2(X) \rightarrow N^+(^3P) + N + e^- \\ N^+(^3P) + 2N_2(X) \rightarrow N_3^+ + N_2 \end{cases}$	AP = 24.3 eV
N_4^+:	$N_2(X) \rightarrow N_2^+ + e^-$ $N_2^+ + 2N_2(X) \rightarrow N_4^+ + N_2$	AP = 15.8 eV

The appearance potentials, AP, were taken from gas-phase experiments and will be somewhat lower in the solid. The first ionization potentials for the primary ion beam gases are as follows: He, 24.5 eV; Ne, 21.6 eV; Ar, 15.8, 15.9 eV; Kr, 14.0, 14.7 eV; Xe, 12.1, 13.4 eV. These numbers show that direct charge transfer can be responsible for the formation of N^+, N_2^+, N_3^+, and N_4^+ ions during He^+ bombardment of a nitrogen matrix but cannot be responsible for the formation of N^+ and N_3^+ during Ar^+ bombardment. The fact that N^+ is more abundant relative to N_2^+ for helium ion bombardment, while the reverse is true for Ar^+ bombardment, suggests that direct charge transfer is important in the formation of this fragment.

The case of N_3^+ is less clear-cut. On basis of the reaction energetics given above, one would expect inelastic momentum transfer rather than direct charge transfer to dominate the formation of N_3^+, by either of the two paths considered. Then, a 4-keV He^+ ion and an 800-eV Ne^+ ion, which have the same momentum, should produce similar relative abundances of N_3^+, and a 4-keV Ar^+ ion should produce a much higher abundance of N_3^+. In reality, the relative N_3^+ yield for an 800-eV Ne^+ beam

(9) V. Čermák and Z. Herman, *Collect. Czech. Chem. Commun.*, **27**, 1493–5 (1962); R. K. Asundi, G. J. Schulz, and P. J. Chantry, *J. Chem. Phys.*, **47**, 1584–91 (1967); T. D. Märk, *Int. J. Mass Spectrom. Ion Phys.*, **9**, 387–95 (1972); *Acta Phys. Aust.*, **37**, 31–7 (1973); M. T. Bowers, P. R. Kemper, and J. B. Laudenslager, *J. Chem. Phys.*, **61**, 4394–9 (1974); T. J. Venanzi and J. M. Schulman, *Mol. Phys.*, **30**, 281–7 (1975); A. Saporoschenko, *Phys. Rev.*, **139**, A352–6 (1965).

(10) J. Gspann and K. Körting, *J. Chem. Phys.*, **59**, 4726–34 (1973).

(11) R. R. Corderman, P. C. Engelking, and W. C. Lineberger, *Appl. Phys.* Lett., **36**, 533–55 (1980).

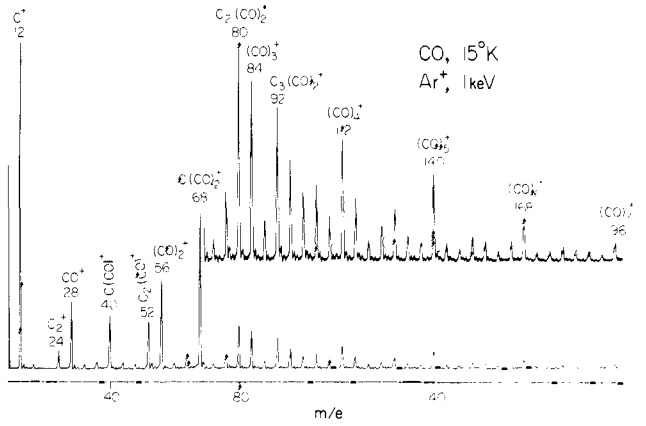

Figure 5. Positive SIMS spectrum of solid CO obtained with a 1-keV Ar^+ beam.

is only a little smaller than that for a 4-keV Ar^+ beam, indicating that the process is more complicated.

Figure 4 gives a logarithmic plot of the cluster ion intensity vs. the cluster size for a cold nitrogen surface bombarded with 4-keV argon ions. Although this result is distorted by the uneven transmission of the quadrupole, which decreases with increasing mass, it is clear that the cluster yield exhibits an approximately exponential decrease as a function of cluster size. A similar behavior was observed before on water.[7]

The data show that the "odd" clusters are less abundant than the "even" ones. In some experiments satellites of the "odd"-cluster signals were observed if a sample was first bombarded with low-energy helium beams and later probed with heavier ions, for example Ar^+ ions. Helium seems to associate with "odd" nitrogen ions to form $(HeN)^+(N_2)_n$ and/or $(HeN_3)^+(N_2)_n$ cluster ions. Spectra of solid N_2 obtained similarly with Ar^+ as primary beam show weak peaks for the known[12] ions ArN^+ and ArN_2^+, as well as a very weak peak for ArN_4^+.

The kinetic energy distribution of the sputtered ions was analyzed. The N^+ and N_2^+ ions have a much wider energy distribution (ca. 20 eV) than the higher clusters (ca. 7 eV or less). A similar difference has been noted for ions vs. cluster ions of water,[7] metals,[13] and alkali halides.[14] It is impossible to measure absolute energy profiles in the present experimental arrangement because of the interaction between the emission current setting of the floodgun (slight under- or overcompensation of the surface charge) and the center band-pass setting of the prefilter. The fact that the lower fragments come off with a wider energy distribution causes their underrepresentation in the recorded spectra because of the relatively small bandwidth admitted to the mass filter.

Carbon Monoxide. Figure 5 shows the SIMS spectrum of frozen CO with a 1-keV Ar^+ beam. Important fragments are C^+, CO^+, C_2O^+, and some C_2^+, whereas O^+ is almost absent. High yields of cluster ions are obtained with compositions $C^+(CO)_n$, $C_2^+(CO)_n$, $CO^+(CO)_n$, etc. Figure 6 shows the SIMS spectrum of solid CO obtained with a 1-keV He^+ beam. Here C^+, O^+, CO^+, and very little C_2^+ are observed and, although some cluster formation takes place, the amount is very small. Except for He^+ beams all other experiments on CO give exceptionally high $C_3O_2^+$ yields. The spectra obtained with Ne^+, Kr^+, and Xe^+ beams were similar to the one obtained with an Ar^+ beam, except that the total cluster yield and the average cluster size increase with the size of the primary ion. An increase of the primary beam energy from 0.5 to 5.0 keV did not change the major features of the spectra but enhanced cluster formation.

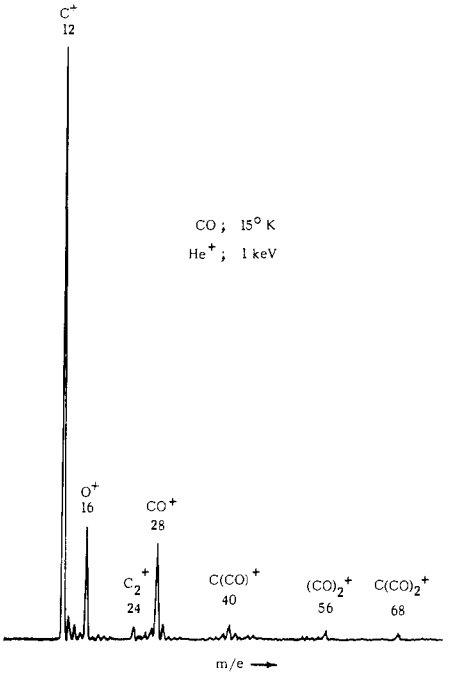

Figure 6. Positive SIMS spectrum of solid CO obtained with a 1-keV He^+ beam.

The three kinds of events described above for solid N_2 can again take place. For CO the following charge-transfer reactions have to be considered:

C^+:	$CO(X) \rightarrow C^+(^2P) + O(^3P) + e^-$	AP = 22.4 eV
O^+:	$CO(X) \rightarrow O^+(^4S) + C(^3P) + e^-$	AP = 24.7 eV
CO^+:	$CO(X) \rightarrow CO^+(X) + e^-$	AP = 14.0 eV
C_2O^+:	$CO(X) \rightarrow CO^+(^4\Sigma) + e^-$ $CO^+(^4\Sigma) + CO(X) \rightarrow C_2O^+ + O(^3P)$	AP = 19.6 eV

C^+ can also be formed by the following inelastic momentum transfer process:

$$CO(X) \rightarrow CO\ (Rydb.)$$
$$CO\ (Rydb.) \rightarrow C^+(^2P) + O^-(^2P) \qquad AP = 20.9\ eV$$

The above appearance potential values were taken from gas-phase experiments[15] and will be somewhat lower in the solid.

The C^+ ion has a high yield in the experiments with He^+ and Ar^+ beams, but its relative yield decreases with a Xe^+ beam. This suggests that both direct charge transfer and inelastic momentum transfer may be responsible for its formation but that the former is the more important. For O^+ the situation is different. This ion is formed essentially only with He^+ as the primary ion. Thus, direct charge transfer seems to be the only mechanism involved here. Another possibility would be that O^+ is formed deep in the solid and, because the ion is very reactive, it will have a high cross section for ion–molecule and association reactions. This last explanation seems less likely since the relative yield of O^+ shows a very small dependence on the kinetic energy of the primary ion beam.

The CO^+ ion can be formed either way because its relative yield is almost independent of the type of primary ion or its energy. The C_2^+ and C_2O^+ ions are typical products of ion–molecule reactions and become more abundant with higher mass and higher kinetic energy primary ions. The $C_3O_2^+$ ion forms a special case because of its dominance in the spectra. The ion–molecule and association reactions which lead to its formation are not understood (possibly $C_2O^+ + CO \rightarrow C_3O_2^+$?).

The CO and N_2 fragments show the same type of kinetic energy distribution. Here the primary formed ions C^+, O^+, and CO^+ have

(12) W. Kaul and R. Fuchs, *Z. Naturforsch., A*, **15a**, 326–35 (1960).
(13) M. A. Rudat and G. H. Morrison, *Surf. Sci.*, **82**, 549–76 (1979).
(14) F. Honda, G. M. Lancaster, Y. Fukuda, and J. W. Rabalais, *J. Chem. Phys.*, **69**, 4931–7 (1978).
(15) C. F. Giese and W. B. Maier, II, *J. Chem. Phys.*, **39**, 197–200 (1963); V. Čermák and Z. Herman, *Collect. Czech. Chem. Commun.*, **30**, 1343–57 (1965); H. Wankenne and J. Momigny, *Chem. Phys. Lett.*, **4**, 132–4 (1969); R. Locht and J. M. Dürer, *ibid.*, **34**, 508–12 (1975).

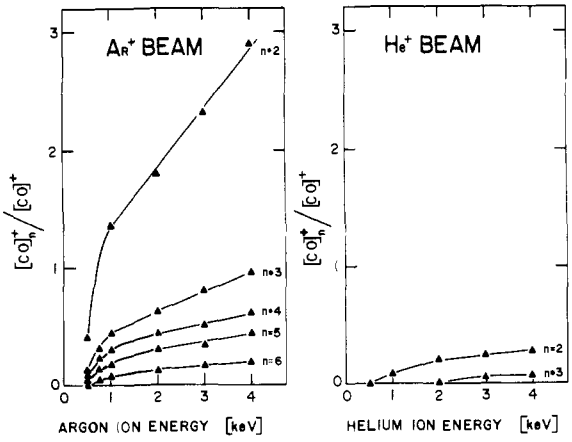

Figure 7. Intensity ratio $(CO)_n^+/(CO)^+$ vs. the kinetic energy of the primary ion for an Ar^+ and He^+ beam.

a much wider energy distribution than the ions formed by ion-molecule reactions or the cluster ions; their average kinetic energy seems to be higher too. Once again, this must be kept in mind when comparing relative ion abundances, since only a relatively small bandwidth is admitted to our mass filter. While the observed qualitative trends are reliable, quantitative values of abundance ratios may be distorted.

In cluster formation solid carbon monoxide behaves similarly to solid nitrogen. Again, the higher the mass and the higher the kinetic energy of the primary ion, the more cluster formation is observed. The formation of clusters of the type $(CO)_n^+$ was studied in more detail. Figure 7 shows the intensity ratio $(CO)_n^+/(CO)^+$ vs. the primary ion kinetic energy for Ar^+ and He^+ beams. These ratios increase almost linearly over the scanned energy range for Ar^+ as primary ion beam. This increase is much less for a He^+ beam, which may be correlated with a higher scattering rate for He^+ ions. In Figure 8 the intensity ratio $(CO)_2^+/(CO)^+$ vs. the momentum of the primary ion is plotted for He^+, Ne^+, Ar^+, and Xe^+ ion beams. The ratio increases most slowly for He^+ and goes up almost in the same way for Ne^+ and Ar^+ with increasing momentum. For Xe^+ ion beams a smaller ratio is measured than the one extrapolated on the basis of momentum. It is not clear how significant this is in view of the possible distortions in the observed values alluded to above.

Flight Time. After the ions and cluster ions leave the solid it takes a few milliseconds before they reach the detector. During this time they may undergo rearrangements or additional fragmentation. Although we were able to change the flight time within a limited range by changing the ion extraction voltages and by increasing the ion velocity along the axis of the quadrupole, we were not able to observe any change in the fragmentation pattern.

Conclusions

One of our goals is to develop SIMS as a supplementary tool for the identification of molecular solids. To accomplish this we have to show that we get secondary ions whose structure is simply related to the composition of the original solid. It is important to get an understanding of the underlying processes of ionization and sputtering.

The results obtained on simple diatomic systems show that the spectra originate from a combination of direct charge transfer, inelastic momentum transfer, and ion–molecule reactions. The probable mechanisms of formation for some fragments were suggested. It was proposed that the extent of cluster formation may be related to the penetration depth of the probe ion in the solid. The stability of the clusters is remarkable. The nitrogen

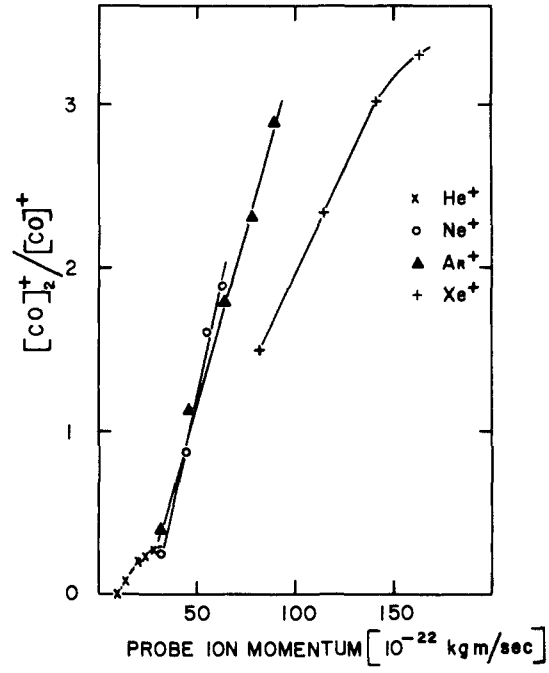

Figure 8. Intensity ratio $(CO)_2^+/(CO)^+$ vs. the momentum of the primary ion for He^+, Ne^+, Ar^+, and Xe^+ ion beams.

clusters are only held together by weak induced dipole and van der Waals forces. For CO the cluster formation is slightly larger, which may be related to the fact that the weak CO dipole moment gives some extra stabilization of the clusters. The lifetime of the clusters is estimated as at least a few milliseconds.

From the point of view of analytical utility, it is disappointing that even simple diatomic molecular solids give rather complicated SIMS spectra. Cluster formation and extensive ion–molecule reactions will make it difficult to use SIMS as a general analytical tool for neat molecular solids since the final spectrum is not simply related to the original composition of the solid. It would be very helpful to use probe ion beams with kinetic energies between 0 and 100 eV because most of the cluster formation and ion–molecule reactions could be eliminated and simpler spectra would be obtained, at the cost of lower sensitivity. As far as we can see, low-energy He^+ primary beams give the most useful results for analytical applications to neat solids, with minimum cluster and ion–molecule product formation. The real analytical power of SIMS for molecular solids is likely to lie in applications to dilute systems in which the species of interest is isolated by a large excess of solid diluent. This situation obtains in surface studies for low coverage of an absorbed species[1] and in matrix-isolation work.[5]

An interesting aspect of SIMS on molecular solids is the possibility of generating intriguing species like N_3^+ and $C_3O_2^+$ which can be mass selected and subjected to various kinds of spectroscopic or controlled-collision experiments. Also cluster ions and association reaction products can be mass selected and studied by other spectroscopic methods.

Acknowledgment. This work was supported by the National Science Foundation (Grant CHE 78-27094) and by NIH Biomedical Research Support Grant No. RR07092. We thank R. G. Orth for many helpful discussions and W. J. Wilcox and J. H. Pitts for superb machining and help in the construction of the instrument. We are also grateful for critical comments by Professor A. L. Wahrhaftig, Professor J. H. Futrell, and Dr. Z. Herman.